Pak. J. Bot., 55(6): 2283-2293, 2023. DOI: http://dx.doi.org/10.30848/PJB2023-6(29)

COMPARATIVE TRANSCRIPTOME ANALYSES REVEALED PHOTOSYNTHESIS- AND SUCROSE METABOLISM-RELATED RESPONSES OF ENDANGERED EVERGREEN TREE SPECIES *PHOEBE BOURNEI* (HEMSL.) YANG – LAURACEAE TO SHADE

XINLIANG LIU, YANFANG WU, LIYAN WANG, YUETING ZHANG, XINGLIN TANG* AND CONG YAN

Jiangxi Academy of Forestry, Jiangxi Nanchang Urban Ecosystem Research Station, Nanchang, Jiangxi, China
**Corresponding author's email: txl_insist@126.com*

Abstract

Phoebe bournei (Hemsl.) Yang of the family Lauraceae is an endangered evergreen ornamental tree species. Shade stress greatly affects the growth and development of *Phoebe* species. To elucidate the molecular mechanisms underlying the shade response, the photosynthesis and transcriptomic profiles of *P. bournei* were examined under shade stress (11.7% light) and full light. The results showed that shade led to a decrease in the net photosynthetic rate (P_n), stomatal conductance (g_s) and transpiration rate (E) of *P. bournei* plants. The shade treatments resulted in a significant increase in plant height and crown diameter. However, diameter at ground level, leaf mass per area (*LMA*), and plant biomass were lower for plants grown under shade conditions than under full light. De novo assembly of RNA sequencing (RNA-seq) data resulted in the generation of 89054 unigenes, and a total of 5404 genes were differentially expressed between the shade treatment and full light. The expression of most differentially expressed genes (DEGs) involved in the photosynthesis antenna pathway was upregulated under shade stress. The downregulated expression of most genes associated with photosynthesis was in agreement with the decreased P_n. The expression of many DEGs related to starch and sucrose metabolism was also significantly affected by shade stress. Our findings provide valuable information for understanding the physiological and molecular regulatory pathways of *P. bournei* in response to shade.

Key words: Light-shading, Gas exchange, Photosynthesis antenna, Starch and sucrose, Plant growth.

Introduction

Phoebe bournei (Hemsl.) Yang is an evergreen broad-leaved tree species in the Lauraceae family. This species is distributed in the mid-subtropical evergreen forests of broad-leaved trees in southeastern China. The wood of *P. bournei*, known as "noble wood", is a valuable material for high-quality furniture and architecture due to the remarkable durability, fragrance, and unique texture (with golden streaks) of the wood (Chen *et al*., 2020a). *Phoebe bournei* is also used as an avenue tree due to its straight trunk and broad crown. However, due to overexploitation, slow growth of the species, and lack of protection, natural populations of *P. bournei* have declined sharply and are listed as national second-class protected plants in China. In recent years, *P. bournei* has been one of the main tree species used for the restoration of subtropical broad-leaved evergreen tree forests in China (Wang *et al*., 2013). Forest canopies lead to reduced understory light levels, which affects the survival and growth of tree seedlings. Thus, studying the shade response of *P. bournei* is very important for its plantation and management in forests.

The morphology, physiology and biochemistry of trees are influenced by shade environment (Samuelson and Stokes 2012; Tang *et al*., 2020a). It has been shown that tree leaves grown under shade conditions exhibit lower leaf mass per area (*LMA*), lower stomatal conductance, lower photosynthetic capacity and higher chlorophyll contents (Piel *et al*., 2002; Tang *et al*., 2020a). Photosynthesis is an important metabolic process for carbohydrate biosynthesis and biomass production in plants. Shading may affect photosynthesis by altering photosynthetic enzyme activity, electron transport chain activity and the amount of light-harvesting pigments (Gharbi *et al*., 2019; Wan *et al*., 2020). It has been reported that photosynthesis of *P. bournei* is influenced by shading (Tang *et al*., 2020a). Additionally, biomass allocation has been shown to be influenced by shading (Raza *et al*., 2020). However, the expression of genes related to photosynthesis and metabolic pathways under shade conditions has not been studied.

The molecular mechanisms underlying plant responses to shade have been successfully explored via RNA sequencing (RNA-seq) technology. Several studies have shown that photosynthesis, pigment biosynthesis, hormone signaling, and starch and sucrose metabolism are transcriptionally regulated during plant adaptation to shading (Ding *et al*., 2016; Shi *et al*., 2019; Chen *et al*., 2020b). Gene expression analysis revealed that light-harvesting complex (LHC) genes in cassava were highly induced by shade, but the expression of starch and sucrose biosynthesis-related genes was decreased (Ding *et al*., 2016). Moreover, genes involved in ATP synthase, electron transport, and the Calvin cycle were shown to be downregulated in rice under low light (Liu *et al*., 2020). On the other hand, some studies have also shown that the expression of LHC genes was inhibited in rice and peanut under shade conditions (Chen *et al*., 2020b; Liu *et al*., 2020). Thus, the expression of photosynthesis-related genes under low light may differ among plant species. It would be important to understand plant responses to shade stress to identify the differentially expressed genes (DEGs) involved in these vital metabolic pathways. However, the molecular mechanism underlying the *P. bournei* response to shade remains unclear.

The aims of this research were to (i) determine the photosynthesis and growth of *P. bournei* in response to shade and (ii) evaluate the transcriptome of *P. bournei* leaves in response to shade. This information will be helpful for improving functional genomics studies of *P. bournei.*

Material and Methods

Plant materials: This experiment was conducted at the Jiangxi Academy of Forestry (115°51′E, 28°41′ N), Nanchang, China. Three-year-old *P. bournei* plants were obtained from the seed-multiplication farm of Xiajiang County (115°19′E, 27°37′ N) in Ji'an, China. Each plant was transplanted into a pot (height of 15 cm and diameter of 18 cm) full of garden soil collected from a 0-20 cm depth. The soil consisted of 31.66 mg kg^{-1} available nitrogen, 52.52 mg kg^{-1} available phosphorus, 78.94 mg kg^{-1} available potassium and 26.79 mg kg^{-1} organic matter.

Shade treatment: At one month after transplantation, uniform plants (height of 50.5-56.3 cm and diameter of 3.74-4.58 mm at ground level) were selected for the shade treatment. A single shade intensity (11.7% of full light; shade) was applied, and each treatment was applied to three plants. To provide shade, a shelter was built with black polyethylene cloth (Angao's, Linyi, China). The control (CK) treatment was applied in parallel under full light. Irradiance under the shade cloth and open-sky conditions was measured with a hand-held leaf fluorometer (FluorPen FP100max, PSI, CZE) at midday in June. Each treatment was replicated four times.

Gas-exchange measurements: An open-flow gas exchange system (Ciras-3, PP Systems, Haverhill, USA) was used to measure leaf gas exchange on sunny days in late September. The leaves were acclimated to the following environment conditions: an ambient CO_2 concentration of 400 μmol mol^{-1}, a photosynthetically active radiation (PAR) of 1200 μmol m^{-2} s^{-1}, a leaf temperature of 26±2°C and a relative humidity of 60±5%. Once a steady state was reached, the net photosynthetic rate (P_n), stomatal conductance (g_s), intercellular CO_2 concentration (C_i) and transpiration rate (E) were measured. Water use efficiency (*WUE*) was calculated as A/E. Three plants were measured for each treatment.

Measurements of plant traits: Plant traits were measured in early October. The plant height, crown diameter and ground diameter were measured. Roots and shoots were collected, separated and dried at 105°C for 30 min followed by 70°C for >72 h until a constant weight was reached. Then, the biomass of the roots, shoots and plants were measured. The root/shoot ratio was considered the ratio of root biomass to shoot biomass. Single-leaf area (S) was determined by a LA-S leaf area meter (WSEEN, Hangzhou, China), and single-leaf dry weight (M) was measured after drying. The leaf mass per area (*LMA*) was calculated as M/S. Three plants were measured for each treatment.

Total RNA isolation, RNA-seq, data analyses, and real-time PCR assays: Whole part of the third to fifth leaf from the top of the plant was used for RNA-seq analysis. Total RNA was extracted from all the leaf samples using a RNeasy Plant Mini Kit (Qiagen, Hilden, Germany) according to the manufacturer's instructions in September. Sequencing libraries were constructed by applying a TruSeq Stranded mRNA kit (Illumina, CA, USA) following the manufacturer's protocol. The RNA-seq library quality was assessed using a Fragment analyzer (Advanced Analytical) and sequenced on an Illumina HiSeq 2500 platform (Illumina, CA, USA). The number of fragments per kilobase of exon per million fragments mapped (FPKM) of unigenes was estimated using RSEM v1.2.15 software to normalize the gene expression levels (Li and Dewey 2011). Genes that were differentially expressed between the CK and shade treatments were analyzed according to the FPKM values of three replicates under shade and full light using DESweq2 software. The screening conditions were p-adjust<0.05 and |log2 (foldchange (FC)|>=1.0. Functional annotation of DEGs was performed using the BLAST program against the following databases: the nonredundant (Nr) protein, SwissProt, Kyoto Encyclopedia of Genes and Genomes (KEGG), Clusters of Orthologous Groups (COG), and Protein family (Pfam) databases. Gene Ontology (GO) enrichment analysis was performed using Blast2GO v2.5 (Götz *et al*., 2008). For real-time PCR, 500 ng of RNA was used to synthesize first-strand cDNA using a Transcriptor First Strand cDNA Synthesis Kit (Roche, Mannheim, Germany). RT-qPCR was performed on an ABI Prism 7500 Sequence Detection System (Applied Biosystems, CA, USA) in conjunction with SYBR Green PCR Master Mix (Takara, China). Actin was used as an internal reference gene. The RT-qPCR data were normalized using the $2^{-\Delta\Delta Ct}$ method for relative quantification (Livak and Schmittgen 2001). Three biological replicates were included for each sample. The names and primer sequences used for the nine genes are listed in (Table S1).

Table S1. Genes and primers used for qRT-PCR.

Gene name	Forward primer (5'-3')	Reverse primer (5'-3')
LHCB1	GTTCTCCATGTTTGGGTTCTT	TCCCACACTTTCACCTCTCT
atpH	TCCATCTCCAATCTCCCCTC	ACTTCCTCTCCATCCCAACC
petF	ATGGGTAAGGCCCTCTTCAG	TTGAGAACCTTTCCGGCACAC
petN	GAGATAGGGGACACGATTCAC	GCGCTTTGCAGAACGATCTA
psbR	CCTCCCTTCTCTTTCAAGGC	CATCGACATTGGCTCCATATT
FBP	TAGCTGATGTCCACCGCAC	AGGAATATGGGAGATCGCTG
RPE	AGCTTCTGCCTGGCAAATCC	CTGCTCGCCCAGCTTTGAA
GAPDH	TGGAGCTGCTGGCGAGATC	TTCGTCGTTGAGAGCAATTCCA
rpiA	GTGGAGTTCGTGGAATCCG	AGATCGACGGCTGGATGAT
Actin	CCTCGACACACAGGCGTTAT	CCATGCTCGATGGGATATTTCA

Table 1. Effects of shade stress on photosynthesis-related parameters of *Phoebe bournei* (means ± SEs).

Treatment	P_n (μmol m^{-2} s^{-1})	g_s (mol m^{-2} s^{-1})	C_i (μmol mol^{-1})	E (mmol m^{-2} s^{-1})	WUE (mmol CO_2 mol^{-1})
CK	9.47 ± 0.03*	0.080 ± 0.003*	245.0 ± 4.7*	1.62 ± 0.06*	5.86 ± 0.20
Shade	7.90 ± 0.21	0.061 ± 0.003	238.0 ± 4.7	1.25 ± 0.06	6.33 ± 0.14

Values are means ± SEs (n = 3). * means differed significantly (p<0.05)

Table 2 Summary of sequence analysis results.

Sample name	Raw reads	Clean reads	Clean bases	Error rate (%)	Q20 (%)	Q30 (%)	GC (%)
CK1	51367738	50927292	7549593767	0.0238	98.51	95.3	47.48
CK2	46163574	45727774	6787049105	0.0239	98.47	95.2	48.49
CK3	42066238	41654848	6209584560	0.024	98.44	95.15	47.65
Shade1	47801318	47257934	7050818505	0.0243	98.31	94.86	47.77
Shade2	43796694	43350662	6448910085	0.0238	98.49	95.31	47.67
Shade3	42937688	42466830	6309340694	0.0242	98.35	94.96	47.55

CK: Full light. Shade: Shade treatment. Q20: Percentage of bases with a Phred value >20. Q30: Percentage of bases with a Phred value >30. GC: Percentage of G and C bases

Table 3. Functional annotations of high-quality unique sequences according to similarity.

Public database	Number of unigenes	Percent (%)
Nr	36479	41.0%
SwissProt	24094	27.1%
GO	31437	35.3%
KEGG	13852	15.6%
COG	28763	32.3%
Pfam	24626	27.7%
Total anno	37285	41.9%
Total	89054	100%

Statistical analyses

Statistical analysis was performed with the R statistical computing environment (R-3.5.1). All data were analyzed using unpaired Student's t-test (p<0.05). Significant differences are indicated with one asterisk (p<0.05). Data are presented as the means ± standard error (SE, n = 3).

Results

Changes in photosynthesis-related parameters and biomass: To determine the effects of shade on photosynthesis, the photosynthesis-related parameters of *P. bournei* were analyzed (Table 1). The P_n and g_s under shade were significantly lower than those under full light, but C_i and *WUE* were not significantly affected by shade treatment. Shade treatment did lead to a significant decrease in the *E*. Several plant traits of *P. bournei* were evaluated (Fig. 1). A significant increase in plant height and crown diameter was found in the shade treatment compared with the CK. The ground diameter, *LMA*, root biomass, shoot biomass, plant biomass and root/shoot ratio of *P. bournei* in the shade treatment were significantly larger than those in the CK.

Transcriptome sequencing and de novo assembly: The cDNA library generated from the RNA of the leaves in the CK and shade groups produced 40.36 Gb of clean nucleotide read data. A pooled cDNA sample from the leaves of *P. bournei* under shading and full light was prepared and sequenced with an Illumina HiSeq 2500. A total of 42066238~51367738 raw reads were generated from the different samples. Adaptor sequences, sequences with ambiguous nucleotides and low-quality sequences were removed using SeqPrep (https://github.com/jstjohn/SeqPrep) and Sickle (https://github.com/najoshi/sickle) software, and 41654848~50927292 clean reads were ultimately obtained.

Using Trinity software (https://github.com/trinityrnaseq/trinityrnaseq/wiki), we assembled a total of 89054 unigenes. The average unigene length was 779 bp, and the N50 length was 1410 bp. Of the 89054 unigenes, 52891 (59.4%) ranged from 200 to 500 bp in length, 16650 unigenes (18.7%) were between 501 and 1000 bp in length, and 19513 unigenes (21.9%) were longer than 1000 bp (Table 2).

Functional annotation of unigenes: In total, 37285 unigenes (41.9%) were successfully annotated via GO, KEGG, COG, NCBI Nr, SwissProt, and Pfam databases (Table 3). Among these 89054 unigenes, 36479 (41.0%), 31437 (35.3%), 13852 (15.6%), 28763 (32.3%), and 24626 (27.7%) unigenes were annotated by the Nr, GO, KEGG, COG, and Pfam databases, respectively. A total of 24094 unigenes (27.1%) were predicted to encode proteins that were identical to proteins in the SwissProt database (Table 3). Based on the alignment of the unigenes from different species in the Nr database, 27345 (75.0%) unigenes had significant hits for *Cinnamomum micranthum* (Hay.) Hay., followed by *Nelumbo nucifera* Gaertn. (771, 2.1%), *Arabidopsis thaliana* (L.) Heynh. (562, 1.5%), *Vitis vinifera* L. (534, 1.5%). Only 19.9% of the annotated unigenes were identified based on unigenes in other plant species (Fig. 2).

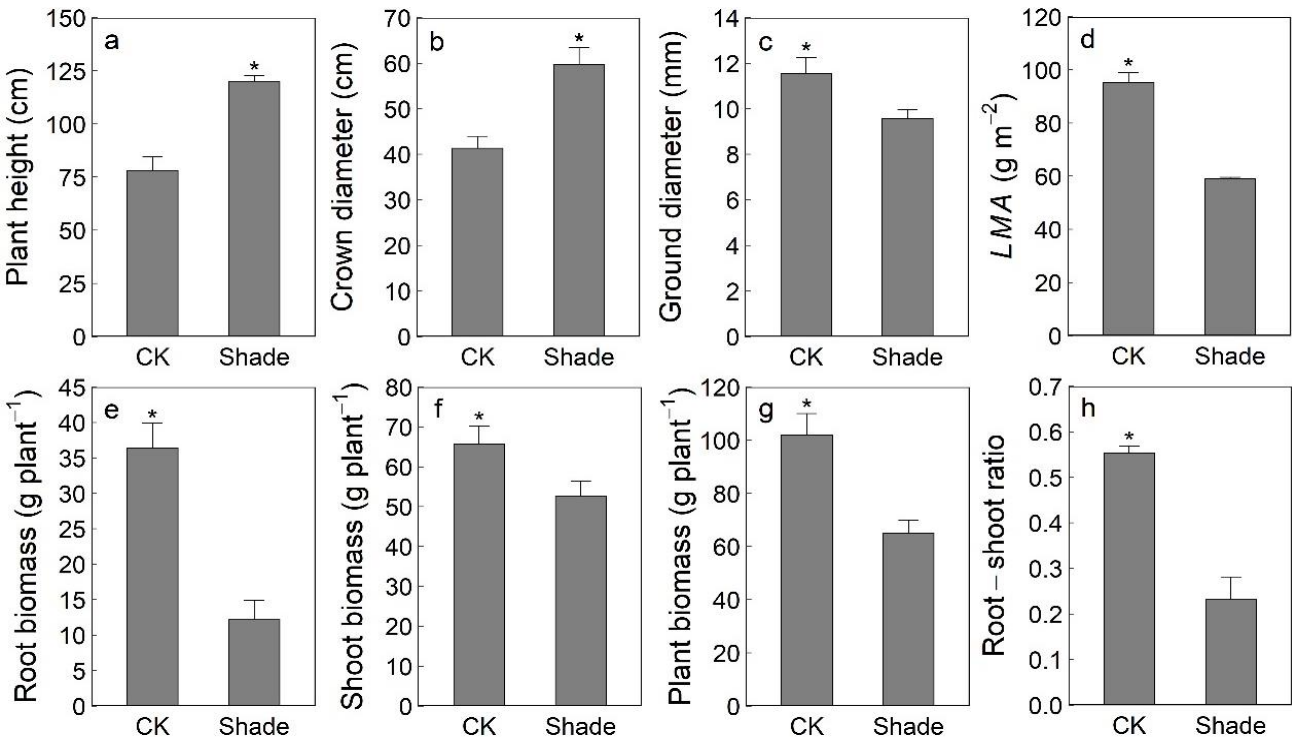

Fig. 1. Effects of shade stress on plant traits and dry matter of *Phoebe bournei* (means±SE) (n = 3). * means differed significantly (p<0.05). *LMA* is the leaf mass per area.

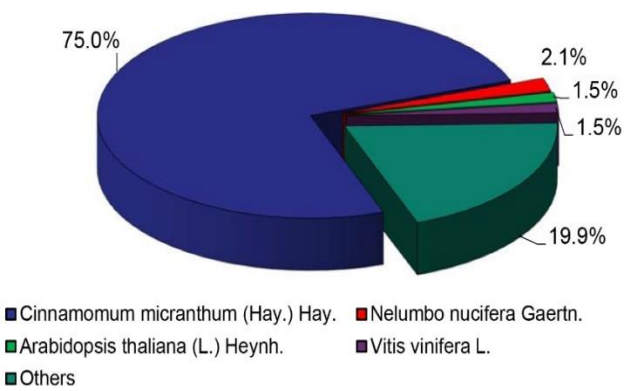

Fig. 2. Alignment of unigenes from different species in the Nr database.

GO and KEGG analysis of genes differentially expressed in response to shading: Overall, 5404 genes (2711 upregulated/3700 downregulated) were differentially expressed between the shade treatment and the CK treatment. GO was used to analyze the functional classifications of the DEGs in the shade treatment. The DEGs were divided according to three main categories: biological processes, cellular components and molecular functions. In the biological process category, cellular process (1163), metabolic process (1096), biological regulation (398), and response to stimulus (385) were prominently represented. For the cellular component category, membrane part (1551), cell part (1266), organelle (672), and membrane (414) were the most abundant subcategories. Within the molecular function category, catalytic activity (1904) and binding (1788) constituted the majority of the category (Fig. 3). These data suggested that the terms "cellular process", "metabolic process", "membrane part", "cell part", "catalytic activity", and "binding" were strongly affected by shading.A total of 25.6% (1424/5572) of the DEGs were annotated via KEGG pathway analysis. The DEGs in the shade treatment were found to be mainly enriched in 122 KEGG pathways. The top 30 KEGG pathways with the highest representation of the DEGs are shown in (Fig. 4). These DEGs were mainly involved in pathways involved in phenylpropanoid biosynthesis; isoquinoline alkaloid biosynthesis; fatty acid elongation; stilbenoid, diarylheptanoid and gingerol biosynthesis; carotenoid biosynthesis; and protein processing in the endoplasmic reticulum.

Regulation of DEGs and their association with photosynthesis: According to the KEGG analysis results, photosynthesis antenna proteins were significantly enriched (Fig. 4). In total, 10 DEGs were identified in the photosynthesis antenna pathway and were annotated to encode the subunits of the light-harvesting chlorophyll protein (LHC) complex (KEGG map ID 00196) (Table 4). Among these DEGs, eight (7 for *LHCB1* and 1 for *LHCB2*) were upregulated, and two (*LHCA5* and *LHCB7*) showed a decrease in expression in the shade treatment compared with the CK.

We further investigated the DEGs involved in the pathways of photosynthesis (Table 5) and carbon fixation in photosynthetic organisms (Table 6). In total, 21 DEGs were annotated in the photosynthesis pathway (10 DEGs) (KEGG map ID 00195) and photosynthetic organism pathway (11 DEGs) (KEGG map ID 00710) (Table 5). Sixteen DEGs showed downregulated expression under

the shade treatment. Among the downregulated DEGs, three (*psbP*, *psbQ* and *psbS*) encoded the subunits of photosystem II (PSII) reaction center pigment-protein complexes; One DEG (*petN*) was involved in the cytochrome b6/f complex; Two DEGs (*petF* and *petH*) and one DEG (delta) functioned in photosynthetic electron transport and the redox chain, respectively; 6 DEGs (one each for *GAPDH*, *GAPA*, *FBP*, *RPE* and two for *FBA*) functioned in the Calvin cycle; and 3 DEGs (*E1.1.1.39*, *GGAT* and *PPDK*) were involved in the C_4-dicarboxylic acid cycle.

Regulation of DEGs involved in starch and sucrose metabolism: Shade-induced DEGs were significantly enriched in the starch and sucrose metabolism pathway. A total of 39 DEGs were induced by the shade treatment (Table S2). Specifically, 11 DEGs were involved in the starch synthesis and decomposition pathways (Table 7). Ten out of eleven DEGs (two for *glgA*, one each for *glgB* and *glgC*, 5 for *WAXY* and 2 for *AMY*) were downregulated. On the other hand, 7 DEGs were involved in the sucrose synthesis and hydrolysis pathways (Table 7). Among them, 5 DEGs (3 for *SUS* and 2 for *malZ*) were significantly upregulated, and two DEGs (*SPP* and *SPS*) were downregulated.

Quantitative real-time PCR (RT-qPCR)-based validation of candidate genes: The expression of 9 candidate DEGs associated with photosynthesis was measured by RT-qPCR (Fig. 5). In response to shade, the expression of 6 genes, i.e., ferredoxin-1 (*petF*), cytochrome b6f complex (cyt b6f complex) subunit 8 (*petN*), ATP synthase delta chain (*atpH*), ribulose-phosphate 3-epimerase (*RPE*), fructose-1,6-bisphosphatase (*FBP*) and glyceraldehyde-3-phosphate dehydrogenase (*GAPDH*), was downregulated, while 3 genes, i.e., chlorophyll a-b binding protein of LHCII type I (*LHCB1*), photosystem II 10 kDa polypeptide (*psbR*) and probable ribose-5-phosphate isomerase 2 (*rpiA*), were upregulated. The similar expression profiles of the candidate DEGs as revealed by RT-qPCR and RNA-Seq confirmed the reliability of the transcriptomic data.

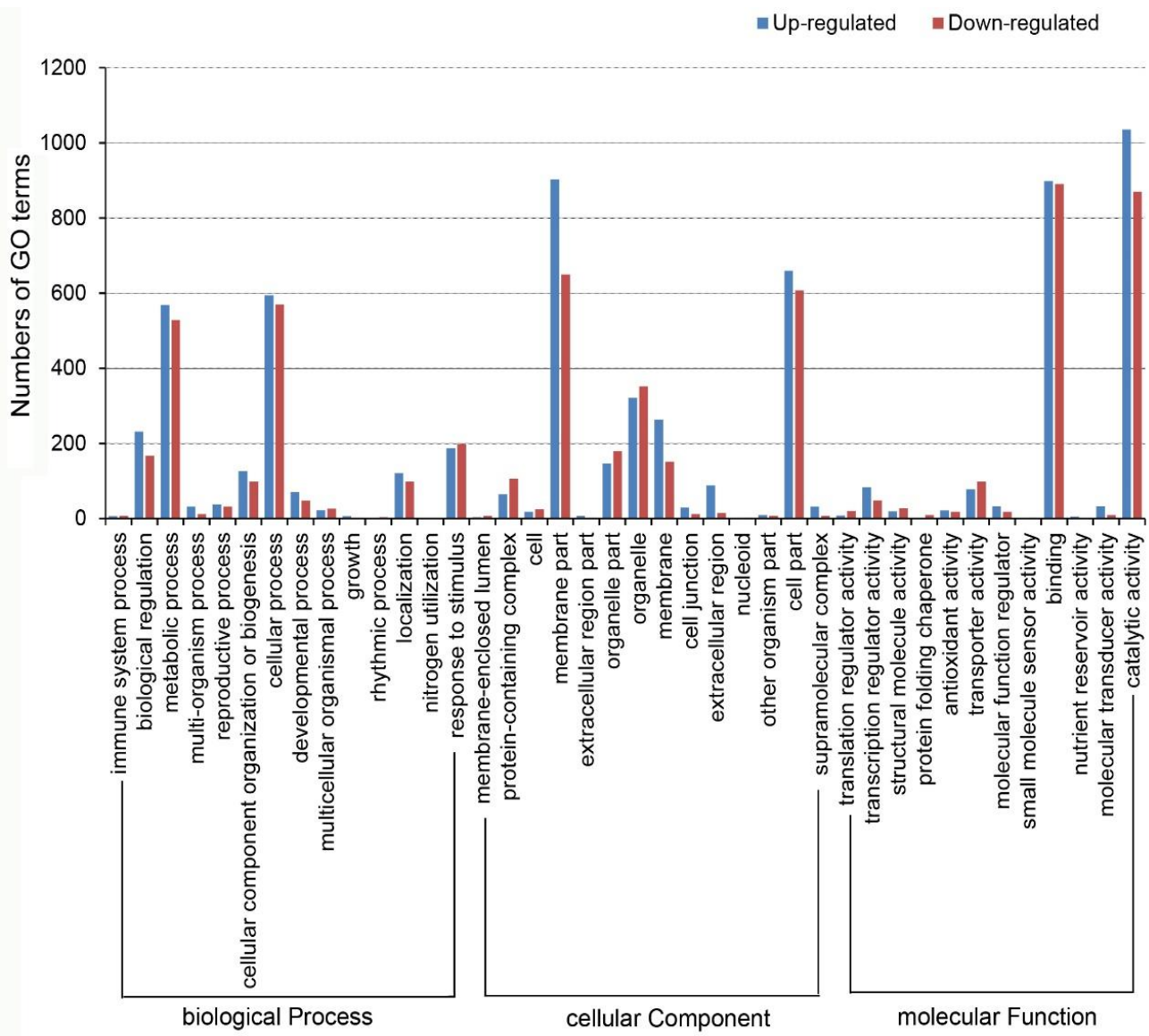

Fig. 3. GO classifications of DEGs in *Phoebe bournei* under shade treatment. The X-axis indicates the number of genes, and the Y-axis indicates the GO terms.

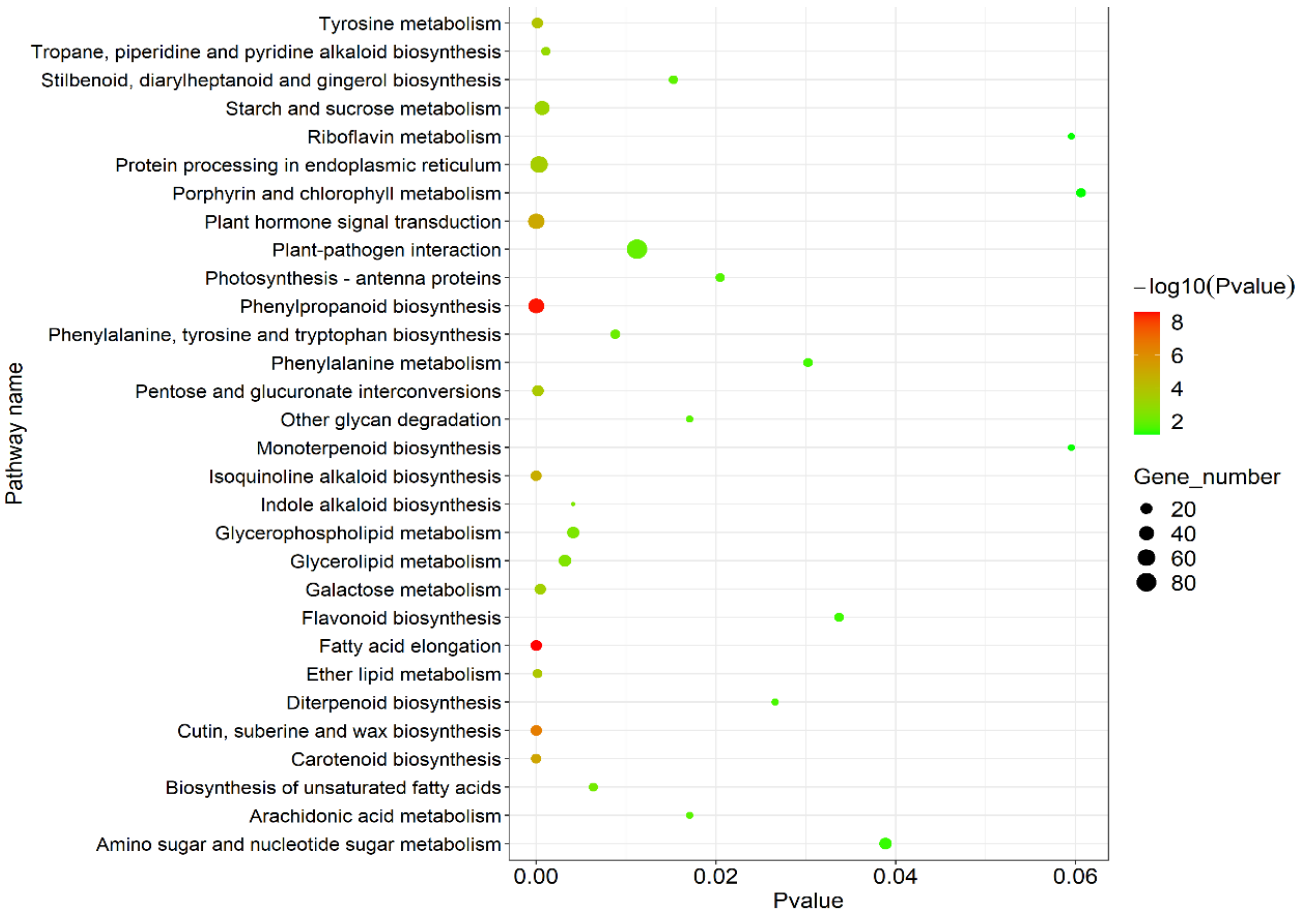

Fig. 4. KEGG enrichment analysis of DEGs in the shade treatment. The richness factor represents the ratio of DEGs to all the annotated genes in the corresponding pathways.

Table 4 Shade stress-induced DEGs and annotations in the photosynthesis antenna pathway.

No.	Gene ID	KO name	Swiss Prot annotation	KO_ID	Up/down
1.	TRINITY_DN429_c0_g1	LHCA5	Photosystem I chlorophyll a/b-binding protein 5	K08911	down
2.	TRINITY_DN965_c0_g1	LHCB1	Chlorophyll a-b binding protein	K08912	up
3.	TRINITY_DN965_c0_g2	LHCB1	Chlorophyll a-b binding protein	K08912	up
4.	TRINITY_DN3188_c0_g1	LHCB1	Chlorophyll a-b binding protein of LHCII type I	K08912	up
5.	TRINITY_DN3188_c0_g2	LHCB1	Chlorophyll a-b binding protein 3	K08912	up
6.	TRINITY_DN5601_c0_g1	LHCB1	Chlorophyll a-b binding protein 3	K08912	up
7.	TRINITY_DN10789_c0_g1	LHCB1	Chlorophyll a-b binding protein of LHCII type I	K08912	up
8.	TRINITY_DN10789_c2_g1	LHCB1	Chlorophyll a-b binding protein	K08912	up
9.	TRINITY_DN3188_c1_g1	LHCB2	Chlorophyll a-b binding protein 151	K08913	up
10.	TRINITY_DN9904_c0_g1	LHCB7	Chlorophyll a-b binding protein 7	K14172	down

Note: The KO names of the genes were obtained from the KEGG database (www.genome.jp/kegg/). The KO_ID represents the ID number of homologs in the KEGG pathway database (www.genome.jp/kegg/)

Table 5. Shade stress-induced DEGs and annotations in the photosynthesis pathway.

No.	Gene ID	KO name	Swiss Prot annotation	KO_ID	Up/down
1.	TRINITY_DN7046_c0_g1	atpH	ATP synthase delta chain	K02113	down
2.	TRINITY_DN13501_c0_g1	petF	Ferredoxin-1	K02639	down
3.	TRINITY_DN32883_c0_g1	petH	Ferredoxin--NADP reductase, leaf isozyme 1	K02641	down
4.	TRINITY_DN14888_c0_g1	petN	Cytochrome b6f complex subunit 8	K03689	down
5.	TRINITY_DN28740_c0_g1	psbP	Photosynthetic NDH subunit of lumenal location 1	K02717	down
6.	TRINITY_DN15316_c0_g1	psbQ	Photosynthetic NDH subunit of lumenal location 3	K08901	down
7.	TRINITY_DN4079_c0_g1	psbS	Photosystem II 22 kDa protein	K03542	down
8.	TRINITY_DN10047_c0_g1	psbR	Photosystem II 10 kDa polypeptide	K03541	up
9.	TRINITY_DN67259_c0_g2	psbR	Photosystem II 10 kDa polypeptide	K03541	up
10.	TRINITY_DN189_c1_g1	psbR	Photosystem II 10 kDa polypeptide	K03541	up

Table 6. Shade stress-induced DEGs and annotations in carbon fixation in photosynthetic organisms.

No.	Gene ID	KO name	Swiss Prot annotation	KO_ID	Up/down
1.	TRINITY_DN58362_c0_g1	GOT2	Aspartate aminotransferase	K14455	up
2.	TRINITY_DN50944_c0_g2	rpiA	Probable ribose-5-phosphate isomerase 2	K01807	up
3.	TRINITY_DN17441_c0_g1	PPDK	Pyruvate, phosphate dikinase	K01006	down
4.	TRINITY_DN3702_c0_g1	GGAT	Glutamate--glyoxylate aminotransferase 2	K14272	down
5.	TRINITY_DN5856_c0_g1	GAPDH	Glyceraldehyde-3-phosphate dehydrogenase	K00134	down
6.	TRINITY_DN11979_c0_g1	GAPA	Glyceraldehyde-3-phosphate dehydrogenase B	K05298	down
7.	TRINITY_DN1876_c0_g1	RPE	Ribulose-phosphate 3-epimerase	K01783	down
8.	TRINITY_DN22211_c0_g1	E1.1.1.39	NAD-dependent malic enzyme 59 kDa isoform	K00028	down
9.	TRINITY_DN5407_c0_g3	FBP	Fructose-1,6-bisphosphatase	K03841	down
10.	TRINITY_DN6757_c0_g1	FBA	Fructose-bisphosphate aldolase, cytoplasmic isozyme 1	K01623	down
11.	TRINITY_DN1688_c0_g1	FBA	Fructose-bisphosphate aldolase 2	K01623	down

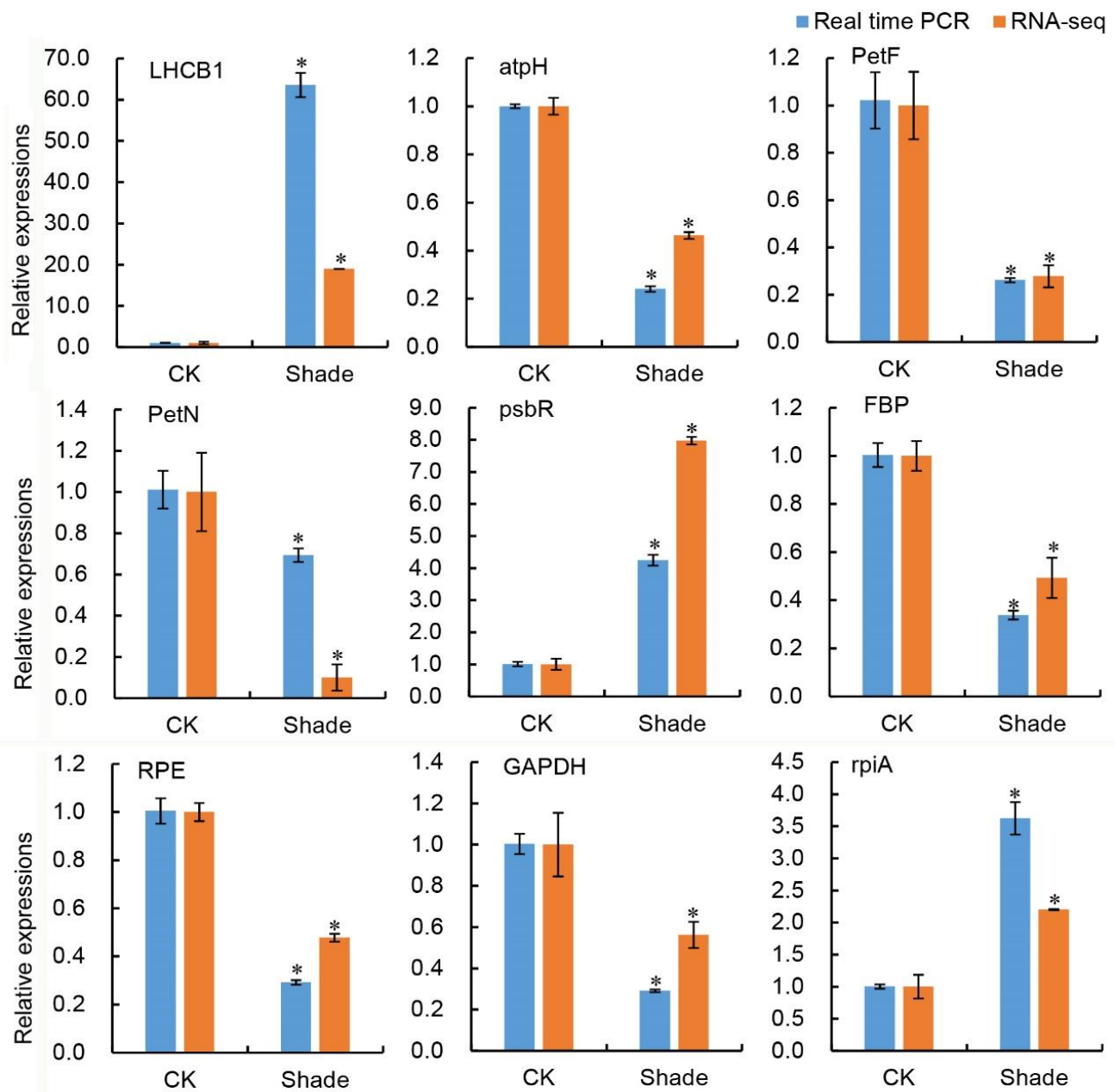

Fig. 5. Real-time PCR results confirmed differentially expressed transcripts identified by RNA-Seq. Nine genes involved in the shade response were selected for validation. Values are means±SEs (n = 3). * means differed significantly (p<0.05). LHCB1: Chlorophyll a-b binding protein of LHCII type I; atpH: ATP synthase delta chain; petF: Ferredoxin-1; petN: Cytochrome b6f complex subunit 8; psbR: Photosystem II 10 kDa polypeptide; FBP: Fructose-1,6-bisphosphatase; RPE: Ribulose-phosphate 3-epimerase; GAPDH: Glyceraldehyde-3-phosphate dehydrogenase; rpiA: Probable ribose-5-phosphate isomerase 2.

Table 7. Shade stress-induced DEGs involved in the synthesis and decomposition of starch or sucrose.

No.	Gene ID	KO name	Swiss Prot annotation	KO_ID	Up/down
1.	TRINITY_DN13982_c0_g1	glgA	Granule-bound starch synthase 2	K00703	down
2.	TRINITY_DN1204_c0_g3	glgA	Granule-bound starch synthase 2	K00703	up
3.	TRINITY_DN11997_c0_g1	glgB	1,4-alpha-glucan-branching enzyme	K00700	down
4.	TRINITY_DN19159_c0_g1	glgC	Glucose-1-phosphate adenylyltransferase	K00975	down
5.	TRINITY_DN709_c0_g1	WAXY	Granule-bound starch synthase	K13679	down
6.	TRINITY_DN26_c0_g1	WAXY	Granule-bound starch synthase	K13679	down
7.	TRINITY_DN709_c1_g1	WAXY	Granule-bound starch synthase	K13679	down
8.	TRINITY_DN709_c1_g2	WAXY	Granule-bound starch synthase	K13679	down
9.	TRINITY_DN48174_c0_g1	WAXY	Granule-bound starch synthase	K13679	down
10.	TRINITY_DN40466_c0_g1	AMY	Alpha-amylase	K01176	down
11.	TRINITY_DN7141_c0_g1	AMY	Alpha-amylase	K01176	down
12.	TRINITY_DN6333_c0_g2	SUS	Sucrose synthase	K00695	up
13.	TRINITY_DN25_c0_g3	SUS	Sucrose synthase	K00695	up
14.	TRINITY_DN25_c0_g2	SUS	Sucrose synthase	K00695	up
15.	TRINITY_DN32679_c0_g2	malZ	Alpha-glucosidase	K01187	up
16.	TRINITY_DN6766_c0_g1	malZ	Alpha-glucosidase	K01187	up
17.	TRINITY_DN5161_c0_g1	SPP	Sucrose-phosphatase	K07024	down
18.	TRINITY_DN5142_c0_g1	SPS	Probable sucrose-phosphate synthase	K00696	down

Table S2. Shade stress-induced DEGs and annotations in starch and sucrose metabolism.

No.	Gene ID	KO name	Swiss Prot annotation	KO_ID	Up/ down
1.	TRINITY_DN32679_c0_g2	malZ	Alpha-glucosidase	K01187	up
2.	TRINITY_DN5360_c0_g1	E2.7.1.4	Fructokinase	K00847	up
3.	TRINITY_DN71039_c0_g1	E3.2.1.4	Endoglucanase 8	K01179	up
4.	TRINITY_DN3598_c0_g1	TPS	Probable alpha,alpha-trehalose-phosphate synthase	K16055	up
5.	TRINITY_DN19159_c0_g1	glgC	Glucose-1-phosphate adenylyltransferase	K00975	down
6.	TRINITY_DN6351_c0_g1	otsB	Trehalose-phosphate phosphatase A	K01087	up
7.	TRINITY_DN66036_c2_g1	E3.2.1.4	Endoglucanase 8	K01179	up
8.	TRINITY_DN1204_c0_g3	glgA	Granule-bound starch synthase 2	K00703	up
9.	TRINITY_DN8475_c0_g1	pgm	Phosphoglucomutase	K01835	down
10.	TRINITY_DN17288_c0_g1	E2.7.1.4	Fructokinase-2	K00847	up
11.	TRINITY_DN3250_c0_g2	E3.2.1.4	Endoglucanase 6	K01179	up
12.	TRINITY_DN11491_c0_g2	E3.2.1.21	Beta-glucosidase	K01188; K05349	up
13.	TRINITY_DN40466_c0_g1	AMY	Alpha-amylase	K01176	down
14.	TRINITY_DN42364_c0_g2	E3.2.1.21	Beta-glucosidase 11	K01188; psom	down
15.	TRINITY_DN6333_c0_g2	SUS	Sucrose synthase	K00695	up
16.	TRINITY_DN1192_c0_g1	E3.2.1.4	Endoglucanase 17	K01179	up
17.	TRINITY_DN1192_c0_g2	E3.2.1.4	Endoglucanase 17	K01179	up
18.	TRINITY_DN67_c0_g1	TPS	Probable alpha,alpha-trehalose-phosphate synthase	K16055	up
19.	TRINITY_DN709_c0_g1	WAXY	Granule-bound starch synthase	K13679	down
20.	TRINITY_DN17278_c0_g1	E3.2.1.4	Endoglucanase 19	K01179	up
21.	TRINITY_DN26_c0_g1	WAXY	Granule-bound starch synthase	K13679	down
22.	TRINITY_DN7631_c0_g1	TPS	Probable alpha,alpha-trehalose-phosphate synthase	K16055	up
23.	TRINITY_DN7252_c0_g1	bglB	Beta-glucosidase 44	K05350	up
24.	TRINITY_DN7141_c0_g1	AMY	Alpha-amylase	K01176	down
25.	TRINITY_DN11997_c0_g1	glgB	1,4-alpha-glucan-branching enzyme	K00700	down
26.	TRINITY_DN13750_c0_g1	E3.2.1.4	------	K01179	down
27.	TRINITY_DN5053_c0_g1	E2.7.1.4	Fructokinase-2	K00847	up
28.	TRINITY_DN13982_c0_g1	glgA	Starch synthase 1	K00703	down
29.	TRINITY_DN709_c1_g1	WAXY	Granule-bound starch synthase	K13679	down
30.	TRINITY_DN709_c1_g2	WAXY	Granule-bound starch synthase	K13679	down
31.	TRINITY_DN5161_c0_g1	SPP	Sucrose-phosphatase	K07024	down
32.	TRINITY_DN48174_c0_g1	WAXY	Granule-bound starch synthase	K13679	down
33.	TRINITY_DN5142_c0_g1	SPS	Probable sucrose-phosphate synthase	K00696	down
34.	TRINITY_DN8576_c0_g1	NUDX14	Nudix hydrolase 14	K18447	down
35.	TRINITY_DN25_c0_g3	SUS	Sucrose synthase	K00695	up
36.	TRINITY_DN25_c0_g2	SUS	Sucrose synthase	K00695	up
37.	TRINITY_DN11816_c0_g1	E3.2.1.4	Endoglucanase 9	K01179	up
38.	TRINITY_DN9464_c0_g1	E3.2.1.21	Beta-glucosidase 31	K01188; mus; pda	up
39.	TRINITY_DN6766_c0_g1	malZ	Alpha-glucosidase	K01187	up

Discussion

Our results showed that shade stress led to significant alterations to both *P. bournei* whole-plant and leaf trait. The plant height and crown diameter of *P. bournei* increased under shade conditions, which could help increase light-harvesting capabilities in low-light environments (Huang *et al*., 2016). *LMA* is a leaf morphological trait, which is mainly dependent on leaf volume and density. *LMA* exhibit a relationship with light uptake, since plants with lower *LMA* have higher leaf area displayed per unit mass invested (hence efficient light capture). In general, trees grown under shade displayed a lower *LMA* (Piel *et al*., 2002), which was similar to our results. Moreover, the P_n, g_s and *E* of *P. bournei* decreased significantly under shade conditions, suggesting that photosynthetic capacity was inhibited by shade stress. The same phenomenon has also been reported in *Boehmeria nivea* (L.) Gaudich. and *Juglans regia* L. (Piel *et al*., 2002; Huang *et al*., 2016).

The photosynthetic pathway plays critical roles in the response to shade. Under shade conditions, some genes assigned to LHC, photosystem I (PSI), PSII, the cytochrome complex and photosynthetic electron transport showed differential expression (Chen *et al*., 2020b). The LHC, which captures radiant energy and transfers light energy to the reaction centers of PSI and PSII, is embedded in the thylakoid membranes of plants. The LHCA and LHCB proteins constitute the antenna systems of PSI and PSII, respectively. The upregulated expression of the DEGs encoding *LHCB1* and *LHCB2* suggested that the adaption of *P. bournei* leaves to shade may be related to the light-harvesting complex, which contrasted with the results of a previous study on *Camellia sinensis* (L.) O. Ktze. (Wu *et al*., 2016). These discrepancies may be due to variation in the shade tolerance of different tree species. Our results are consistent with those of earlier research showing that *P. bournei* leaves grown in shade environment exhibit higher PSII maximum efficiency (F_v'/F_m') (Tang *et al*., 2020b). *LHCB7* plays a role in the pH-dependent balance of electron transport, which influences Rubisco turnover (Peterson and Schultes 2014). *LHCB7* was downregulated in response to shade, which could reduce carbon assimilation capacity. Moreover, *LHCA5* has a role in heat dissipation and thereby in the photoprotection of PSI; *LHCA5* was downregulated in *P. bournei* under shade conditions, which was in agreement with the findings of a previous report on *A. thaliana* (Ganeteg *et al*., 2004). In higher plants, *psbO*, *psbP* and *psbQ* are extrinsic proteins of the oxygen-evolving complex (OEC) of PSII of eukaryotes; these proteins are bound to the luminal surface of the PSII complex (Suorsa *et al*., 2006). *psbO* proteins have been found to play a stabilization role within the manganese cluster (Nagao *et al*., 2010). Experimental evidence suggests that *psbP* and *psbQ* play important roles in optimizing oxygen-evolving activity by regulating the binding of proteins with Cl^- and Ca^{2+} cofactors (Pagliano *et al*., 2009; Nagao *et al*., 2010). It has been shown that the *psbR* protein plays a role in maintaining the structural stability of PSII and is crucial for the stable assembly of the *psbP* and *psbQ* proteins (Suorsa *et al*., 2006). *psbS* has been shown to regulate nonphotochemical quenching (*NPQ*), which protects the photosynthetic machinery from high light through the thermal dissipation of excess light energy (Głowacka *et al*., 2018). According to the KEGG pathway analysis, under shade conditions, *psbP*, *psbQ* and *psbS* were downregulated; *PsbR* was upregulated; and no difference in expression was observed for *psbO*. It has been reported that shade resulted in a significant decrease in the q_P, *NPQ*, and *ETR* of *P. bournei* (Tang *et al*., 2020b). Based on previous studies, we conclude that downregulated expression of key PSII genes in the leaves of *P. bournei* under shade conditions may be an important factor for the decreased PSII photochemical efficiency and limited electron transport ability.

PetF encodes ferredoxin, which plays a vital role in electron transfer between PSI and ferredoxin-NADPH-oxidoreductase (*FNR*) (Tognetti *et al*., 2006). Overexpression of *petF* can increase the scavenging efficiency of reactive oxygen species in chloroplasts to alleviate damage to organelles under high light (Tognetti *et al*., 2006). *FNR*, which is encoded by the *petH* gene, catalyzes the terminal step in light-driven electron transfer from ferredoxin or flavodoxin to $NADP^+$ at PSI (Lu *et al*., 2020). The *petN* protein is a genuine subunit of the cyt b6f complex and plays a crucial role in the assembly and/or stability of the complex (Hager *et al*., 1999). Shade led to the downregulation of the *petF*, *petH* and *petN* genes, thereby inhibiting photosynthetic electron transport and reducing the production of NADPH for carbon fixation. In addition, the *atpH* gene, which encoded an F-type ATPase, was downregulated under shade treatment suggesting that ATP synthesis was seemingly inhibited and that less energy (ATP) was provided for carbon fixation. Together, these results suggested that altered expression of DEGs involved in photosynthesis pathways under shade treatment led to a decrease in photosynthetic activity.

The Calvin cycle, the main biosynthetic pathway of carbon fixation in C_3 plants, plays a vital role in metabolism for plant growth. Our transcriptome sequencing results showed that most genes encoding proteins involved in the Calvin cycle were downregulated under shade conditions. The *GAPDH* and *GAPA* genes, whose products catalyze the reversible conversion of 1,3-bisphosphoglycerate into glyceraldehyde-3-phosphate, were downregulated. A similar trend was also observed in rice (Liu *et al*., 2020). The expression of *RPE*, whose protein catalyzed the interconversion of ribulose-5-phosphate and xylulose-5-phosphate, was also downregulated (Kopp *et al*., 1999). *FBP*, which catalyzes the hydrolysis of fructose-1,6-bisphosphate to fructose-6-phosphate and inorganic phosphate, is one of the key enzymes in the Calvin cycle (Ge *et al*., 2020). Previous studies have revealed that *FBP* plays a vital role in plant responses to abiotic stresses such as drought and salt (Ge *et al*., 2020). Fructose-1,6-bisphosphate aldolase (*FBA*) is an essential enzyme in the Calvin cycle that catalyzes the reversible conversion of fructose-1,6-bisphosphate to glyceraldehyde 3-phosphate and dihydroxyacetone phosphate (Oelze *et al*., 2014). Previous studies have indicated that the *FBA* gene plays an important role in the response to various stresses, such as salinity, drought and

light acclimation (Fan *et al*., 2009; Oelze *et al*., 2014). In the present study, the decreased expression of the *FBP* and *FBA* genes in the leaves of *P. bournei* under shade conditions may result in decreased sucrose synthesis, eventually inhibiting photosynthesis.

Starch and sucrose metabolism plays pivotal roles in plant growth and stress responses. Many intermediates of carbohydrates, the precursor components of biomass, are provided by sucrose and starch metabolism (Chen *et al*., 2020b). In the current work, several genes were found to be involved in starch synthesis and decomposition. Glucose-1-phosphate adenylyltransferase (*glgC*), which catalyzes the transfer of alpha-D-glucose-1-phosphate to ADP-glucose, is the key enzyme responsible for regulating starch biosynthesis (Weigelt *et al*., 2009). 1,4-Alpha-glucan branching enzyme (*glgB*) and granule-bound starch synthase (*WAXY*) play important roles in starch biosynthesis. *glgB* mainly catalyzes the conversion of amylose to starch, and *WAXY* mainly contributes to the synthesis of amylose (Han *et al*., 2019). Alpha-amylase (*AMY*), which catalyzes the cleavage of alpha-1,4-glycosidic linkages in starch and glycogen compounds, plays a central role in the regulation of starch degradation (Huang *et al*., 2021). Thus, the downregulation of *glgC, glgB, WAXY* and *AMY* in the leaves of *P. bournei* under shade conditions indicates reduced synthesis and hydrolysis of starch. On the other hand, several genes involved in sucrose synthesis and hydrolysis were identified. Sucrose synthase (*SUS*) catalyzes the reversible reaction of sucrose and uridine diphosphate (UDP) into UDP-glucose and fructose and plays important roles in stress responses (Li *et al*., 2020). D-Fructose-6P is converted to sucrose via the actions of sucrose-6-phosphate synthase (*SPS*) and sucrose-6-phosphate phosphatase (*SPP*) (Maloney *et al*., 2015). It has also been proposed that sucrose synthesis is largely catalyzed by a multienzyme complex involving both *SPS* and *SPP*, whereas sucrose breakdown is generally catalyzed by *SUS* (Huber and Huber 1996). Moreover, it has been shown that alpha-glucosidase (*malZ*) is important in sucrose decomposition (Kalita *et al*., 2018). As observed in our study, the downregulated expression of the *SPS* and *SPP* genes indicated that sucrose synthesis in the leaves was inhibited under shade. In addition, genes encoding *SUS* and *malZ* were upregulated, suggesting that sucrose decomposition in the leaves increased under shade.

Conclusion

In summary, shade stress increases plant height and crown diameter but decreases diameter at ground level, *LMA*, and plant biomass. In addition, the P_n and g_s were significantly decreased in response to shade. By comparing the expression of DEGs in associated pathways, we found that the expression of photosynthesis antenna-related genes was upregulated but that most of the genes involved in the photosynthesis and carbon fixation pathways were downregulated. In addition, many DEGs involved in starch and sucrose metabolism were also significantly affected by shade stress.

Acknowledgment

This research was funded by the Key Research and Development Program of Jiangxi Province (20203BBF62W010) and the Research Project of Jiangxi Forestry Bureau (202207 and 202115).

References

Chen, S., W. Sun, Y. Xiong, Y. Jiang, X. Liu, X. Liao, D. Zhang, S. Jiang, Y. Liu, B. Liu, L. Ma, X. Yu, L. He, B. Liu, J. Feng, L. Feng, Z. Wang, S. Zou, S. Lan and Z. Liu. 2020 a. The phoebe genome sheds light on the evolution of magnoliids. *Hortic. Res.*, 7: 146.

Chen, T., H. Zhang, R. Zeng, X. Wang and L. Zhang. 2020 b. Shade effects on peanut yield associate with physiological and expressional regulation on photosynthesis and sucrose metabolism. *Int. J. Mol. Sci.*, 21: 5284.

Ding, Z., Y. Zhang, Y. Xiao, F. Liu, M. Wang, X. Zhu, P. Liu, Q. Sun, W. Wang, M. Peng, T. Brutnell and P. Li. 2016. Transcriptome response of cassava leaves under natural shade. *Sci. Rep.*, 6: 31673.

Fan, W., Z. Zhang, Y. Zhang. 2009. Cloning and molecular characterization of fructose-1,6- bisphosphate aldolase gene regulated by high-salinity and drought in *Sesuvium portulacastrum*. *Plant Cell Rep.*, 28: 975-984.

Ganeteg, U., F. Klimmek and S. Jansson. 2004. Lhca5 – an LHC-type protein associated with photosystem I. *Plant Mol. Biol.*, 54: 641-651.

Ge, Q., Y. Cui, J. Li, J. Gong, Q. Lu, P. Li, Y. Shi, H. Shang, A. Liu, X. Deng, J. Pan, Q. Chen, Y. Yuan and W. Gong. 2020. Disequilibrium evolution of the Fructose-1,6-bisphosphatase gene family leads to their functional biodiversity in *Gossypium* species. *B.M.C. Genom.*, 21: 379.

Gharbi, F., A. Guizani, L. Zribi, H.B. Ahmed and F. Mouillot. 2019. Differential response to water deficit stress and shade in two wheat (*Triticum durum* Desf.) cultivars: Growth, water relations, osmolyte accumulation and photosynthetic pigments. *Pak. J. Bot.*, 51(4).

Głowacka, K., J. Kromdijk, K. Kucera, J. Xie, A.P. Cavanagh, L. Leonelli, A.D.B. Leakey, D.R. Ort, K.K. Niyogi and S.P. Long. 2018. Photosystem II Subunit S overexpression increases the efficiency of water use in a field-grown crop. *Nat. Comm.*, 9: 868.

Götz, S., J.M. García-Gomez, J. Terol, T.D. Williams, S.H. Nagaraj, M.J. Nueda, M. Robles, M. Talon, J. Dopazo and A. Conesa. 2008. High-throughput functional annotation and data mining with the Blast2GO suite. *Nucl. Acids Res.*, 36: 3420-3435.

Hager, M,, K. Biehler, J. Illerhaus, S. Ruf and R. Bock. 1999. Targeted inactivation of the smallest plastid genome-encoded open reading frame reveals a novel and essential subunit of the cytochrome b6f complex. *Embo J.*, 18: 5834-5842.

Han, H., C. Yang, J. Zhu, L. Zhang, Y. Bai and E. Li. 2019. Competition between granule bound starch synthase and starch branching enzyme in starch biosynthesis. *Rice*, 12: 96.

Huang, C.J., G. Wei, Y.C. Jie, J.J. Xu, S.A. Anjum and M. Tanveer. 2016. Effect of shade on plant traits, gas exchange and chlorophyll content in four ramie cultivars. *Photosynthetica*, 54: 390-395.

Huang, P., C. Li, H. Liu, Z. Zhao and W. Liao. 2021. Hydrogen gas improves seed germination in cucumber by regulating sugar and starch metabolisms. *Horticulturae*, 7: 456.

Huber, S.C. and J.L. Huber. 1996. Role and regulation of sucrose-phosphate synthase in higher plants. *Ann. Rev. Plant Physiol. Plant Mol. Biol.*, 47: 431-444.

Kalita, D., D.G. Holm, D.V. LaBarbera, J.M. Petrash and S.S. Jayanty. 2018. Inhibition of α-glucosidase, α-amylase, and

aldose reductase by potato polyphenolic compounds. *Plos One,* 13:e0191025.

Kopp, J., S. Kopriva, K. Suss and G.E. Schulz. 1999. Structure and mechanism of the amphibolic enzyme d-ribulose-5-phosphate 3-epimerase from potato chloroplasts. *J. Mol. Biol.*, 287: 761-771.

Li, B. and C.N. Dewey. 2011. RSEM: accurate transcript quantification from RNA-Seq data with or without a reference genome. *B.M.C. Bioinform.*, 12: 323.

Li, J., K. Gao, B. Lei, J. Zhou, T. Guo and X. An. 2020. Altered sucrose metabolism and plant growth in transgenic *Populus tomentosa* with altered sucrose synthase PtSS3. *Transg. Res.*, 29: 125-134.

Liu, Y., T. Pan, Y. Tang, Y. Zhuang, Z. Liu, P. Li, H. Li, W. Huang, S. Tu,G. Ren, T. Wang and S. Wang. 2020. Proteomic analysis of rice subjected to low light stress and overexpression of *OsGAPB* increases the stress tolerance. *Rice*, 13: 30.

Livak, K.J. and T.D. Schmittgen. 2001. Analysis of relative gene expression data using real-time quantitative PCR and the $2^{-\Delta\Delta CT}$ *Method. Methods*, 25: 402-408.

Lu, H., J. Cheng, Z. Wang, X. Zhang, S. Chen and J. Zhou. 2020. Enhancing photosynthetic characterization and biomass productivity of nannochloropsis oceanica by nuclear radiation. *Front. Energy Res.*, 8: 143.

Maloney, V.J., J. Park, F. Unda and S.D. Mansfield. 2015. Sucrose phosphate synthase and sucrose phosphate phosphatase interact in planta and promote plant growth and biomass accumulation. *J. Exp. Bot.*, 66: 4383-4394.

Nagao, R., T. Suzuki, A. Okumura, A. Niikura, M. Iwai, N. Dohmae, T. Tomo, J. Shen, M. Ikeuchi and I. Enami. 2010. Topological analysis of the extrinsic PsbO, PsbP and PsbQ proteins in a green algal PSII complex by cross-linking with a water-soluble carbodiimide. *Plant Cell Physiol.*, 51: 718-727.

Oelze, M.L., M. Muthuramalingam, M. Vogel and K.J. Dietz. 2014. The link between transcript regulation and de novo protein synthesis in the retrograde high light acclimation response of *Arabidopsis thaliana*. *BMC Genom.*, 15: 320.

Pagliano, C., N.L. Rocca, F. Andreucci, Z. Deak, I. Vass, N. Rascio and R. Barbato. 2009. The extreme halophyte *Salicornia veneta* is depleted of the extrinsic PsbQ and PsbP proteins of the oxygen-evolving complex without loss of functional activity. *Ann. Bot.*, 3: 505-515.

Peterson, R.B. and N.P. Schultes. 2014. Light-harvesting complex B7 shifts the irradiance response of photosynthetic light-harvesting regulation in leaves of *Arabidopsis thaliana*. *J. Plant Physiol.*, 171: 311-318.

Piel, C., E. Frak, X.L. Roux and B. Genty. 2002. Effect of local irradiance on CO_2 transfer conductance of mesophyll in walnut. *J. Exp. Bot.*, 53: 2423-2430.

Raza, M., L. Feng, N. Iqbal, I. Khan and W. Yang. 2020. Effects of contrasting shade treatments on the carbon production and antioxidant activities of soybean plants. *Fun. Plant Biol.*, 47: 342-354.

Samuelson, L.J. and T.A. Stokes. 2012. Leaf physiological and morphological responses to shade in grass-stage seedlings and young trees of longleaf pine. *Forests*, 3: 684-699.

Shi, Q., F. Kong, H. Zhang, Y. Jiang, S. Heng, R. Liang, L. Ma, J. Liu, X. Lu, P. Li and G. Li. 2019. Molecular mechanisms governing shade responses in maize. *Biochem. Bioph. Res. Co.*, 516: 112-119.

Suorsa, M., S. Sirpio, Y. Allahverdiyeva, V. Paakkarinen, F. Mamedov, S. Styring and E. Aro. 2006. PsbR, a missing link in the assembly of the oxygen-evolving complex of plant photosystem II. *J. Biol. Chem.*, 281: 145-150.

Tang, X., G. Liu, J. Jiang, B. Liu, Y. Zhang and L. Di. 2020b. Effects of shading on the chlorophyll fluorescence characteristics and light energy partitioning of one-and three-year-old *Phoebe bournei* seedlings. *Chinese J. Ecol.*, 39: 3247-3254.

Tang, X., G. Liu, J. Jiang, C. Lei, Y. Zhang, L. Wang and X Liu. 2020a. Effects of growth irradiance on photosynthesis and photorespiration of *Phoebe bournei* leaves. *Fun. Plant. Biol.*, 47: 1053-1061.

Tognetti, V.B., J.F. Palatnik, M.F. Fillat, M. Melzer, M.R. Hajirezaei, E.M. Valle and N. Carrillo. 2006. Functional replacement of ferredoxin by a cyanobacterial flavodoxin in tobacco confers broad-range stress tolerance. *Plant Cell*, 18: 2035-2050.

Wan, Y., Y. Zhang and M. Zhang. 2020. Shade effects on growth, photosynthesis and chlorophyll fluorescence parameters of three *Paeonia* species. *Peer J.*, 8: e9316.

Wang, W., X. Wei, W. Liao, J.A. Blanco, Y. Liu, S. Liu, G. Liu, L. Zhang, X. Guo and S. Guo. 2013. Evaluation of the effects of forest management strategies on carbon sequestration in evergreen broad-leaved (*Phoebe bournei*) plantation forests using FORECAST ecosystem model. *Forest Ecol.*, *Manag.*, 300: 21-32.

Weigelt, K., H. Kuster, T. Rutten, A. Fait, A.R. Fernie, O. Miersch, C. Wasternack, R.J. Emery, C. Desel, F. Hosein, M. Muller, I. Saalbach and H. Weber. 2009. ADP-glucose pyrophosphorylase-deficient pea embryos reveal specific transcriptional and metabolic changes of carbon-nitrogen metabolism and stress responses. *Plant Physiol.*, 149: 395-411.

Wu, Q., Z. Chen, W. Sun, T. Deng and M. Chen. 2016. De novo sequencing of the leaf transcriptome reveals complex light-responsive regulatory networks in *Camellia sinensis* cv. *Baijiguan*. *Front. Plant Sci.*, 7: 332.

(Received for publication 27 July 2022)